Ⓔ

Model Update May 2016: Upper-Mantle Heterogeneity beneath North America from Travel-Time Tomography with Global and USArray Data

by Scott Burdick, Frank L. Vernon, Vladik Martynov, Jennifer Eakins, Trilby Cox, Jonathan Tytell, Taimi Mulder, Malcolm C. White, Luciana Astiz, Gary L. Pavlis, and Robert D. van der Hilst

ABSTRACT

P-wave travel-time residuals from USArray helped improve the scale and consistency with which the mantle beneath North America is resolved. Beginning in 2008, we published a series of *P*-wave velocity models based on a global ray theoretical inversion of USArray and global catalog data. Here, we present the final model update, MITP_2016MAY, which includes the complete set of travel-time residuals from USArray Transportable Array (TA) in the contiguous United States. In this model, the area of high resolution extends to the eastern margin of the continent, allowing us to better estimate the location and extent of slow features in Central Virginia and New England. An increasing number of data from the TA in Alaska also allows us to recover the structure of subducting Pacific plate and Yakutat terrane. In addition to highlighting new features in the final model, we visualize and discuss the improvements to the model due to the addition of USArray data through time.

Electronic Supplement: MATLAB MITP_2016MAY model and plotting scripts, figures of checkerboard tests, and animations of model evolution.

INTRODUCTION

As of May 2016, the deployment of USArray Transportable Array (TA; see Data and Resources), the seismological component of EarthScope (see Data and Resources), in the contiguous United States has ended. The installation of the TA continues in Alaska, where recording began in 2011. Data from USArray now enable the imaging of seismic structure beneath the eastern margin of North America and parts of Alaska with hitherto unseen scope and resolution. In previous research notes (Burdick *et al.*, 2008, 2009, 2010, 2012, 2014), we presented 3D tomographic models of mantle *P* wavespeed from global and USArray travel-time data recorded through November 2007, December 2008, January 2010, March 2011, and January 2013, respectively. Here, we present the final model of the series, MITP_2016MAY, which has been updated with USArray travel-time picks through May 2016. Although we describe the new major features present in the update, a full interpretation of the model is beyond the scope of this brief research note. However, we discuss the evolution of the MITP_2016MAY models and include, as an Ⓔ electronic supplement to this article, visualizations of the month-by-month effects of adding USArray data to the tomographic inversion.

METHODOLOGY AND DATA

We performed a global inversion of *P*-phase travel-time residuals from USArray (TA, Reference Network, and Cascadia Initiative stations) and global catalogs. The tomographic problem is linearized using rays traced in the 1D reference model ak135 (Kennett *et al.*, 1995) on a regular grid. The model grid is adapted in response to the distribution of ray paths by iteratively merging poorly sampled mantle volumes, and optimal model is solved for using least-squares method (Paige and Saunders, 1982) with smoothing and weak norm damping. The resulting model of *P*-wave velocity variations MITP_2016-MAY is given as percent difference from ak135 at each depth. A full description of the tomographic method used can be found in Li *et al.* (2008).

The dataset comprises over 10 million *P* travel times from the International Seismological Centre and the National Earthquake Information Center (hereafter, Engdahl–van der Hilst–Buland [EHB] dataset) processed using the algorithms

doi: 10.1785/0220130186

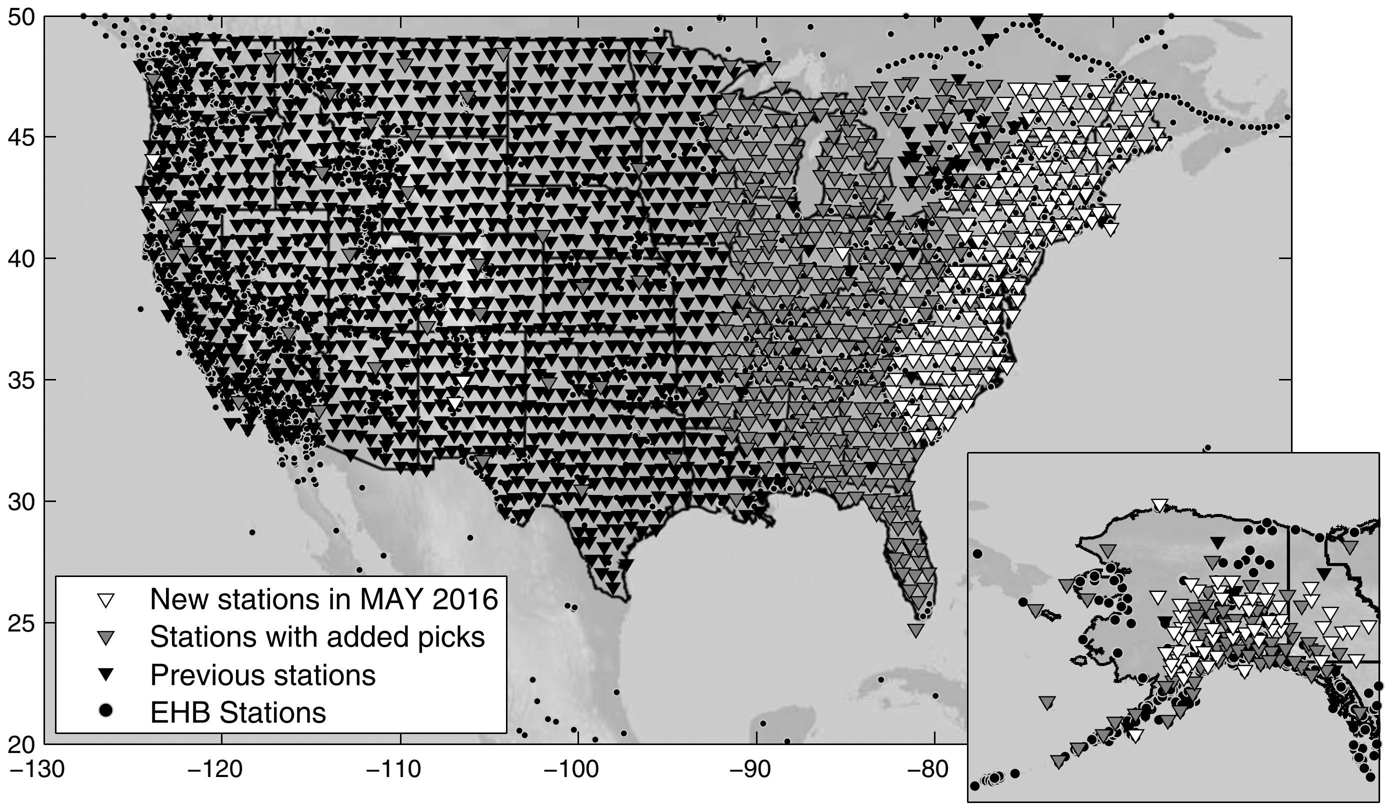

▲ **Figure 1.** Geographical distribution of stations in and around the United States used in the inversion. Black dots represent stations contributing to the Engdahl–van der Hilst–Buland (EHB) dataset; the worldwide station distribution is depicted in Li *et al.* (2008). Black and gray triangles represent USArray station locations from the previous model update for data through January 2013 (Burdick *et al.*, 2014). Gray stations have additional picks made after the previous update. White triangles represent the new USArray stations included in the dataset.

developed by Engdahl *et al.* (1998), combined with a database of over 3,210,000 USArray travel times (see Data and Resources). The USArray travel times, handpicked at the Array Network Facility (ANF), have been shown to have lower variance than the travel times drawn from global databases (Burdick and Lekic, 2016). As of May 2016, the ANF has added over 560,000 new *P*-wave travel-time residuals from teleseismic and upper-mantle distances (14°–100°) originating from 6130 events occurring between January 2013 and May 2016. Of the new residuals, some 120,000 are from stations in and around Alaska. The updated set includes data recorded at 200 new USArray station locations along the East Coast and 120 stations in Alaska (Fig. 1), in addition to new data from stations included in the Midwest and Gulf Coast states recorded after January 2013.

The initial model grid has a spacing of $0.35° \times 0.35° \times 45$ km worldwide. Improvements to the grid (Fig. 2) due to the addition of ray paths from new events are most significant eastward of the Appalachian range and beneath the Gulf of Mexico, where the adaptive grid now retains the smallest spacing. To capture structure newly illuminated by the extension of the TA to Alaska, we also begin with a fine gridding in that region. The adaptive grid algorithm maintains the smallest spacing beneath the current extent of the array and Aleutian arc.

EVOLUTION OF THE MITP MODEL

Between 2007 and 2014, we published a series of five global *P*-wave models with fine parametrization in the continental United States adapted in response to added USArray picks. The value of the USArray project is demonstrated by the progressive improvements to the resolution of seismic structure beneath the array. Here, we give a brief overview of improvements attained through successive iterations.

Prior to the deployment of USArray, North America was populated by a combination of sparse global and national networks and small-scale arrays targeting local structure and seismicity. The coverage was irregular between regions—extremely dense along the San Andreas fault system and other tectonically active areas in the west and sparse or nonexistent in large areas east of the Rocky Mountains. The initial model created without USArray data (presented in Burdick *et al.*, 2008) detected low velocities and small-scale variations in the west and an undifferentiated high-velocity body extending to 400 km depth beneath the center of the United States. The recovery of the Juan de Fuca slab and Yellowstone was detailed at shallow depths, but resolution was lost in the transition zone and below. On the eastern margin, the Great Meteor hotspot and

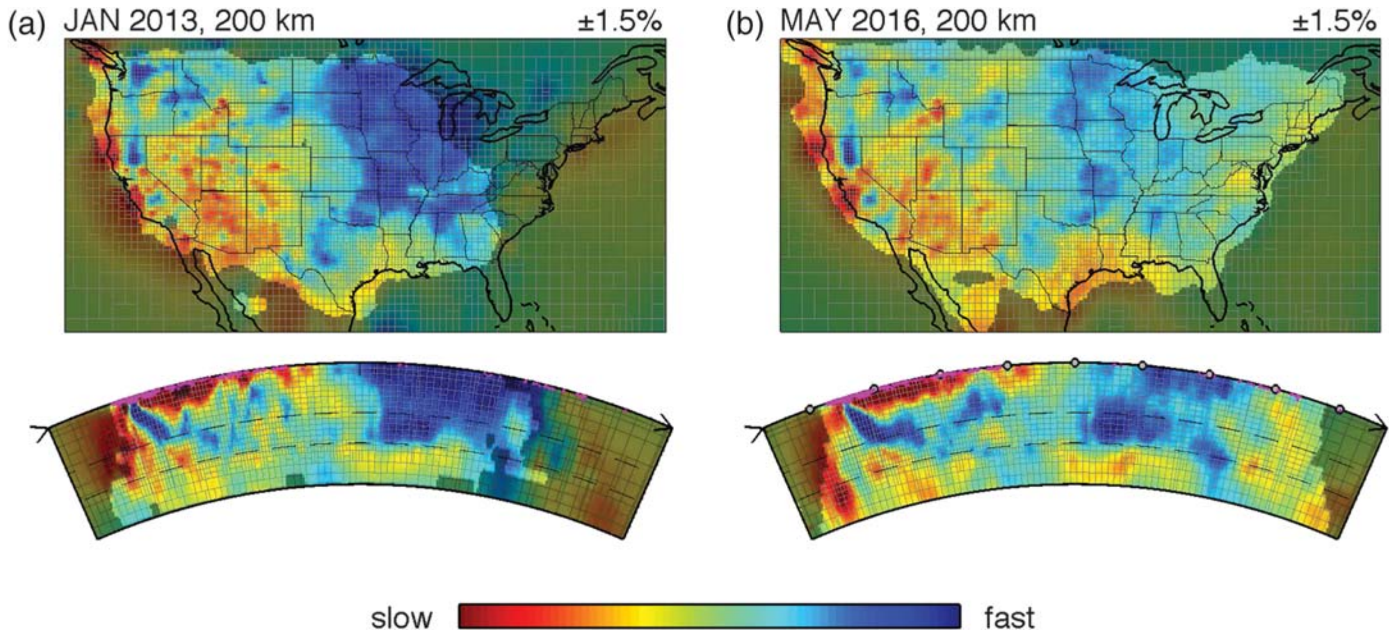

▲ **Figure 2.** Illustration of grid refinement. Map views at 200 km depth and cross sections illustrating the grids used for the 2013 and 2016 models (on a and b, respectively). *P*-wave velocities are given as percent difference from ak135, with the range specified on each plot. Cross sections run at 40° N from −130° to −70° W down to 1000 km depth, with dashed black lines marking 410 and 660 km. Shaded areas indicate locations where 1.5° checkerboard is not recovered. The majority of refinements are made beneath regions with stations added after the 2013 update, but the western part of the model continues to update based on redeployed Transportable Array stations and events around the western margin.

Central Virginia anomaly appeared as broadly distributed slow areas.

The first model to include USArray data, MITP_2007-NOV (Burdick *et al.*, 2008) was created by adding around 600,000 *P* picks from stations extending from the west coast inland to 110° W, covering much of the Basin and Range, Colorado plateau, and northern Rockies. Although much of the footprint of the array was already densely sampled in the EHB dataset in many places, refinements were made in the northwest and Basin and Range. The Cascadia subduction was revealed as a thin high-velocity zone from Vancouver to the Mendocino Triple Junction, and the slow anomaly due to the Yellowstone hotspot was brought into relief with the adjacent fast Wyoming craton.

As the array moved into the Rocky Mountains, MITP_2008DEC (Burdick *et al.*, 2009) added 390,000 USArray picks. Continued data collection in the northwest improved the imaging of along-strike variation in the Cascades subduction, including a robust decrease in wavespeed beneath the High Lava Plains in Oregon. Variation within the Colorado plateau also became apparent, with a well-defined transition between the fast interior and slower regions abutting the Basin and Range.

In the next update, data from USArray began to improve resolution on the stable platform of the continent. MITP_2010JAN (Burdick *et al.*, 2010) added 280,000 *P* picks from stations extending into the Great Plains. The heterogeneity in the upper mantle beneath the plains states had a smaller degree of variation than in the tectonically active west, but fine structure was revealed around the Black Hills and in Central Texas. The data began to distinguish between high wavespeeds due to the cold cratonic lithosphere and those of underlying features inferred to be remnants of the Farallon subduction.

MITP_2011MAR (Burdick *et al.*, 2012) included some 260,000 new *P* picks from USArray stations ranging from Gulf Coast to the Superior Province. This update further indicated that variations exist among different tectonic blocks in the stable center of the continent. The fast signature of the cratonic lithosphere becomes stronger and more confined laterally. The fast anomalies beneath the Ouachita Mountains and Ozark plateau came into focus. With an increase in the number of crossing rays, the signature of the Farallon slab in the transition zone beneath the Great Plains became stronger and more compact.

The most recent *P*-wave model, MITP_2013JAN (Burdick *et al.*, 2014) added nearly two years of additional USArray data, including more than 900,000 *P* picks from stations extending throughout the entire Gulf Coast, the Central Lowlands, the western Appalachians, and Ontario. This update illuminated the affects of ancient and ongoing rifting in the center of the continent. A relatively slow linear feature in the top 100 km coincides with the gravitational anomaly due to the Midcontinental rift. Below the New Madrid seismic zone and Reelfoot rift lie slow structures extending beyond 200 km depth.

To visualize the effects that USArray has on the recovery of mantle structure, we create a series of models through time. From the inception of the array to May 2016, we add cumulative USArray data in one-month increments to the inversion on the

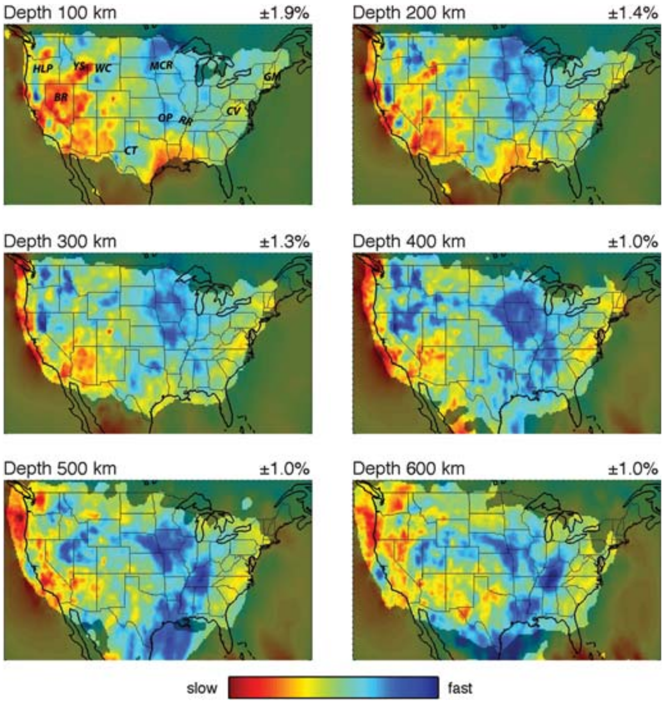

▲ **Figure 3.** Lateral variations in *P*-wave velocity according to model MITP_2016MAY at 100, 200, 300, 400, 500, and 600 km depth in the mantle beneath the continental United States. Shaded areas indicate locations where 1.5° checkerboard is not recovered. Prominent features are marked: High Lava Plains (HLP), Yellowstone (YS), Basin and Range (BR), Wyoming craton (WC), central Texas (CT), Ozark plateau (OP), Reelfoot rift (RR), Midcontinental rift (MCR), Great Meteor hotspot (GM), and Central Virginia anomaly (CV).

final adaptive grid. The resulting models, viewed in order, show the dramatic improvement in illumination through time and provide better sense of the effects of specific parts of the array. Animated figures of cross sections, maps, and checkerboard resolution tests are included the Ⓔ electronic supplement.

WHAT IS NEW?

The final model MITP_2016MAY allows for the evaluation of the entire contiguous United States with roughly uniform resolution. Figures 3 and 4 depict upper-mantle heterogeneity beneath the contiguous United States. To obtain a measure of where seismic structure is recovered, we perform checkerboard resolution tests (Ⓔ Figs. S3–S4). The results of the tests are used to calculate the resolving power of the inversion, as defined in Burdick *et al.* (2014). In Figures 2–5, shaded regions indicate places where the checkerboard is not recovered (resolving power is below a threshold value of 0.65). Resolving power indicates that the data are able to recover 1.5° × 1.5° structure in the upper mantle everywhere beneath the United States with the exception of Florida, where the aperture is too narrow at shallow depths. Although the most notable changes to the model occur where new stations improve resolution, the western part of the model continues to evolve (Fig. 2), due to the continued accumulation of data at inherited TA stations in the west, the introduction of new ray paths from events from the western margin recorded at new stations in the east, and a minor reduction in the relative effect of regularization.

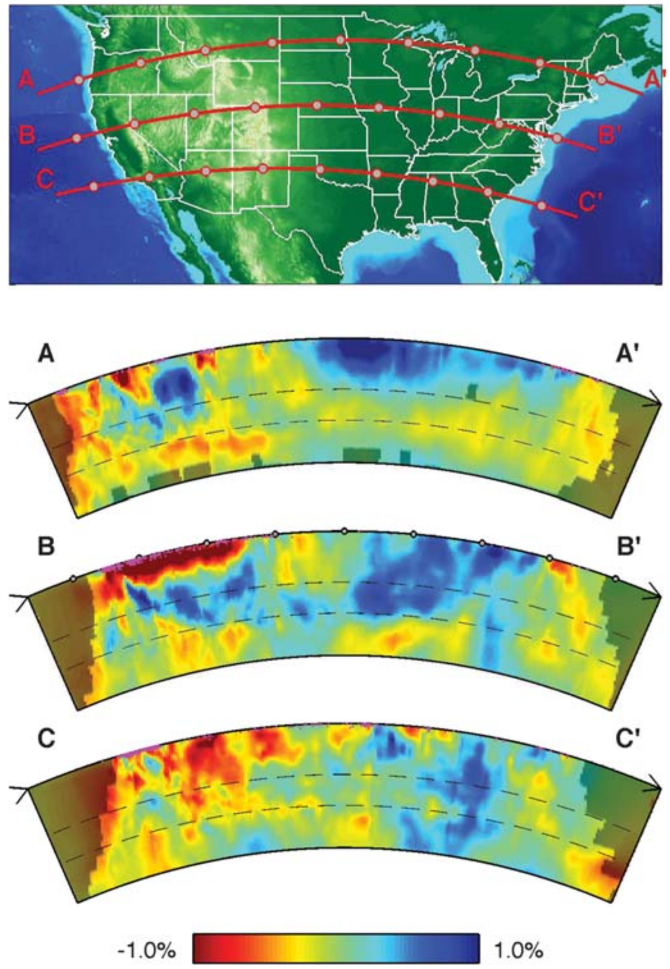

▲ **Figure 4.** Cross sections through the model down to 1000 km. Dashed lines represent 410 and 660 km depth. Note that cross sections are now resolved with 1.5° resolution to the eastern margin of the continent.

Prior to the inversion, residuals from USArray stations had a standard deviation of 1.11 s compared to travel times calculated in ak135. The correction due to mantle structure in MITP_2016MAY resulted in a variance reduction of 51%. Residuals from the global catalogs had a standard deviation of 1.6 s, and their variance was reduced by only 15%, suggesting that the USArray picks are more self-consistent. Regional variations in variance reduction for the USArray residuals can be found in Ⓔ Figure S5. For a quantitative treatment of variance in *P*-wave travel times from USArray and global datasets and the uncertainty in the recovery of mantle velocity beneath North America, see Burdick and Lekic (2016).

In general, heterogeneity in the upper 400 km east of the Appalachians is of lower amplitude than beneath the craton and the western United States. The scale of variations is similar

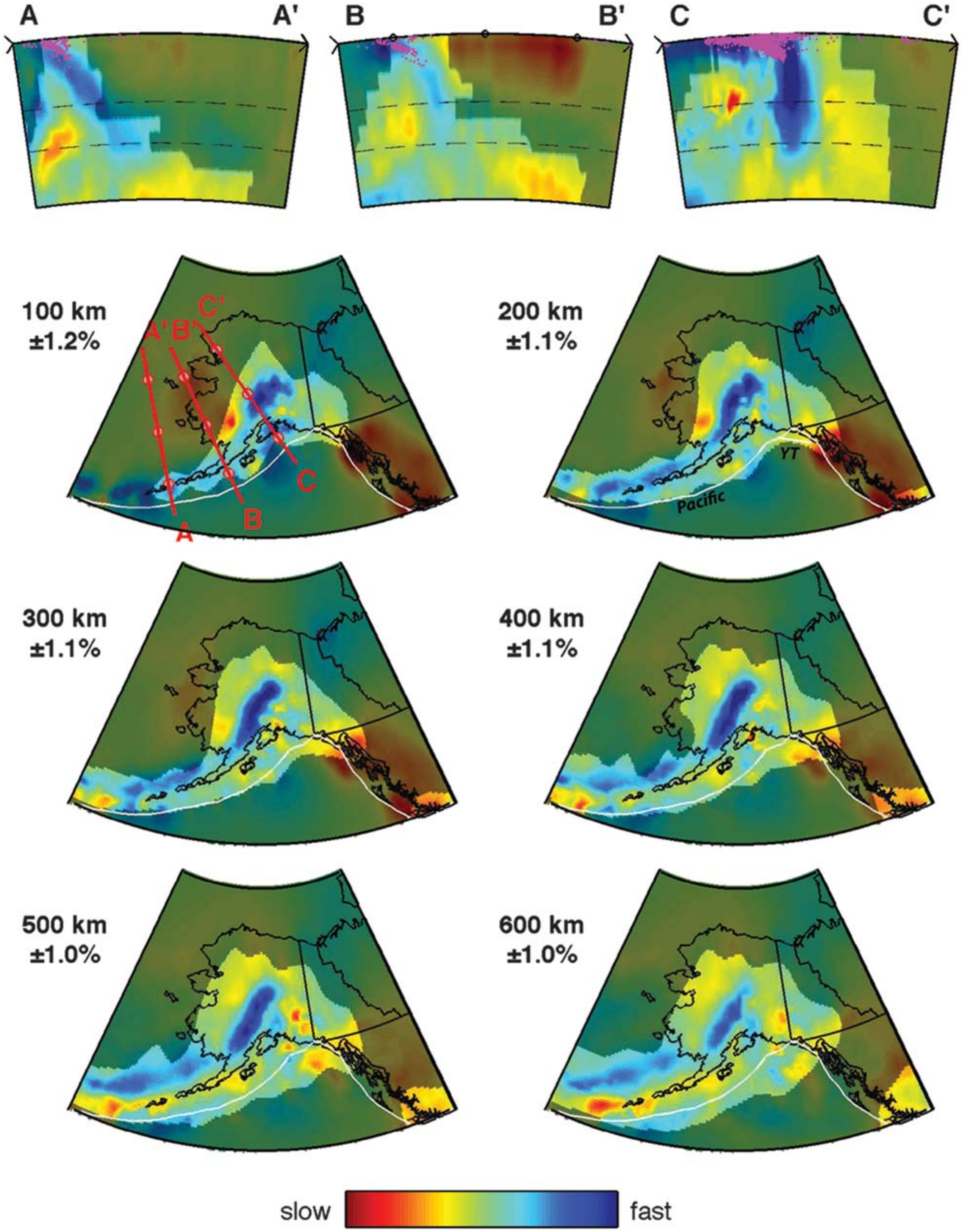

▲ **Figure 5.** *P*-wave velocity variations in and around Alaska. Cross sections extend to 1000 km with dashed lines at 410 and 660 km depth. The locations of the sections are given by the red lines on the top left map section. Maps show lateral variations in *P* wavespeed at from 100 to 600 km depth. Shaded areas indicate locations where 3° checkerboard is not recovered. White lines denote the plate boundaries, with the location of the Yakutat terrane (YT) marked on the 200-km depth map. Pink dots represent earthquakes of magnitude 5.3 or greater.

to that beneath the center of the continent, save for two notable small-scale features. Beneath Central Virginia, the data resolve a 0.5% reduction in velocity coincident with anomalous Cenozoic volcanism at the surface (Chu *et al.*, 2013). Below 300 km, the anomaly merges into an elongated southwest-trending slow feature that extends to Georgia. In northern New England, we detect a slow structure related to the Great Meteor hotspot track (Villemaire *et al.*, 2012; Boyce *et al.*, 2016). At depths greater than 200 km, the anomaly spreads to the southeast off the coast of Massachusetts before resolution is lost. The slow anomalies in Virginia and New England were present in previous model updates, but the addition of new data allows us to constrain their spatial extent to be less than 2° in diameter in the upper mantle.

The transition zone beneath the eastern half of the continent is dominated by fast anomalies commonly inferred to be related ancient subduction. With the addition of data from the eastern margin, the separation between cratonic mantle and underlying fast heterogeneity became more distinct (Fig. 2). The most prominent fast anomaly lies between 500 and 700 km depth beneath Kentucky and has been variously interpreted as evidence of lithospheric downwelling (Biryol *et al.*, 2016) or the stagnation of the Farallon slab (Schmandt and Lin, 2014). We find that this feature is spatially connected with other fast anomalies to the west and deeper anomalies to the east.

With the extension of USArray to Alaska and adjacent regions of Canada, which began in 2011, new data provided details about the subduction of the Pacific plate and Yakutat terrane. Figure 5 shows sections through MITP_2016MAY beneath mainland Alaska and the Aleutian arc. Resolving power tests indicate that 3° × 3° structure can be resolved within the southeastern half of Alaska in the upper 200 km and beneath the entire state at transition zone depths. Although the Aleutians remain sparsely instrumented, resolution of structure beneath them is provided earthquakes originating in the subduction zone and recorded elsewhere.

In the upper 200 km, we find slab geometry similar to that recovered by surface-wave tomography (Wang and Tape, 2014) and regional body-wave tomography (Eberhart-Phillips *et al.*, 2006; Martin-Short *et al.*, 2016). The subducted Pacific plate shows as a long linear fast feature beginning in central Alaska with a sharp kink as it extends west beneath the Aleutians. The fast slab anomaly is well correlated with local seismicity, with the seismicity ceasing south of the eastern edge. In the upper mantle beneath the Aleutians (Fig. 5, sections A and B), the slab dips at an angle between 20° and 30° from normal before appearing to flatten out in the transition zone, although the resolution is lost north of the intersection of the slab and the 660 km discontinuity. Resolution tests also show significant smearing of the subduction signature outside of the continent, so the uniformity of the slab along strike between 400 and 500 km may be artificial. Beneath the continent (Fig. 5, section C), the slab signature becomes stronger and broader, and the dip goes nearly vertical, ending at ~660 km depth. The eastern termination of the high-velocity feature that we presume marks the subducting slab terminates in central Alaska. The eastern edge of that anomaly is consistent with the regional model of Martin-Short *et al.* (2016).

CONCLUDING REMARKS

In this research note, we present the *P*-wave velocity model MITP_2016MAY that includes more than 3,210,000 *P*-wave travel-time residuals from 2004 through May 2016 obtained from nearly 2000 USArray seismograph sites.

The addition of three years of travel-time picks from the ANF improved the resolution of finescale structure beneath the Appalachians, Eastern margin, and Alaska in comparison to the result of Burdick *et al.* (2014). The new data help refine the location and extent of anomalously slow regions in Virginia and New England related to past episodes of volcanism and shows a link between the Cascadia subduction zone and fast anomalies beneath the southeast. Improved resolution beneath Alaska and the Aleutian arc also enables detailed investigation of the subduction of the Pacific plate and Yakutat terrane.

Model MITP_2016MAY and scripts for making horizontal and vertical cross sections through it are available as an Ⓔ electronic supplement, which also includes two sets of animations. The first visualizes the 3D geometry of the model by plotting vertical slices through the contiguous United States in a direction approximately parallel to Farallon-North America plate motion averaged over the past 30 Ma. The second explores the effects of month-by-month addition of USArray data.

DATA AND RESOURCES

The *P*-phase residuals from USArray used in this study are available to the community as CSS monthly files from the Array Network Facility (ANF) http://anf.ucsd.edu/tools/events/download.php. *P* residuals from the Engdahl–van der Hilst–Buland (EHB) Bulletin are available at http://www.isc.ac.uk/ehbbulletin/. Data from USArray Transportable Array are from http://www.iris.edu/USArray, and the seismological component of EarthScope are from http://www.earthscope.org.

ACKNOWLEDGMENTS

The authors thank the USArray team for their superb efforts in array installation and data quality control and the Incorporated Research Institutions for Seismology for continued excellence and leadership in data storage and dissemination. Data used in this study were made available through EarthScope (www.earthscope.org; EAR-0323309), supported by the National Science Foundation (NSF). The construction and dissemination of our model updates is supported by NSF Grant EAR-1349771.

REFERENCES

Biryol, C. B., L. S. Wagner, K. M. Fischer, and R. B. Hawman (2016). Relationship between observed upper mantle structures and recent tectonic activity across the southeastern United States, *J. Geophys. Res.* **121,** no. 5, 3393–3414, doi: 10.1002/2015JB012698.

Boyce, A., I. D. Bastow, F. A. Darbyshire, A. G. Ellwood, A. Gilligan, V. Levin, and W. Menke (2016). Subduction beneath Laurentia modified the eastern North American cratonic edge: Evidence from *P* wave and *S* wave tomography, *J. Geophys. Res.* **121,** no. 7, 5013–5030, doi: 10.1002/2016JB012838.

Burdick, S., and V. Lekic (2016). Velocity variations and uncertainty from transdimensional *P*-wave tomography of North America, *Geophys. J. Int.* (in revision).

Burdick, S., R. D. Hilst, F. Vernon, V. Martynov, T. Cox, J. Eakins, T. Mulder, L. Astiz, and G. Pavlis (2009). Model update December 2008: Upper mantle heterogeneity beneath North America from travel time tomography with global and USArray Transportable Array data, *Seismol. Res. Lett.* **80,** 638–645.

Burdick, S., C. Li, V. Martynov, T. Cox, J. Eakins, T. Mulder, L. Astiz, F. L. Vernon, G. L. Pavlis, and R. D. van der Hilst (2008). Upper mantle heterogeneity beneath North America from travel time tomography with global and USArray Transportable Array data, *Seismol. Res. Lett.* **79,** 384–390.

Burdick, S., R. D. van der Hilst, F. L. Vernon, V. Martynov, T. Cox, J. Eakins, G. H. Karasu, J. Tylell, L. Astiz, and G. L. Pavlis (2010). Model update January 2010: Upper mantle heterogeneity beneath North America from traveltime tomography with global and USArray Transportable Array data, *Seismol. Res. Lett.* **81,** no. 5, 689–693.

Burdick, S., R. D. van der Hilst, F. L. Vernon, V. Martynov, T. Cox, J. Eakins, G. H. Karasu, J. Tylell, L. Astiz, and G. L. Pavlis (2012). Model update March 2011: Upper mantle heterogeneity beneath North America from traveltime tomography with global and USArray Transportable Array data, *Seismol. Res. Lett.* **83,** no. 1, 23–28.

Burdick, S., R. D. van der Hilst, F. L. Vernon, V. Martynov, T. Cox, J. Eakins, G. H. Karasu, J. Tylell, L. Astiz, and G. L. Pavlis (2014). Model update January 2013: Upper mantle heterogeneity beneath North America from travel-time tomography with global and USArray Transportable Array data, *Seismol. Res. Lett.* **85,** no. 1, 77–81.

Chu, R., W. Leng, D. V. Helmberger, and M. Gurnis (2013). Hidden hotspot track beneath the eastern united states, *Nature Geosci.* **6,** no. 11, 963–966.

Eberhart-Phillips, D., D. H. Christensen, T. M. Brocher, R. Hansen, N. A. Ruppert, P. J. Haeussler, and G. A. Abers (2006). Imaging the transition from Aleutian subduction to Yakutat collision in central Alaska, with local earthquakes and active source data, *J. Geophys. Res.* **111,** no. B11303, doi: 10.1029/2005JB004240.

Engdahl, E. R., R. van der Hilst, and R. Buland (1998). Global teleseismic earthquake relocation with improved travel times and procedures for depth determination, *Bull. Seismol. Soc. Am.* **88,** no. 3, 722–743.

Kennett, B. L. N., E. R. Engdahl, and R. Buland (1995). Constraints on seismic velocities in the Earth from travel-times, *Geophys. J. Int.* **122,** no. 1, 108–124.

Li, C., R. D. van der Hilst, E. R. Engdahl, and S. Burdick (2008). A new global model for P wave speed variations in Earth's mantle, *Geochem. Geophys. Geosyst.* **9,** no. Q05018, doi: 10.1029/2007GC001806.

Martin-Short, R., R. M. Allen, and I. D. Bastow (2016). Subduction geometry beneath south central Alaska and its relationship to volcanism, *Geophys. Res. Lett.* **43,** 9509–9517.

Paige, C. C., and M. A. Saunders (1982). LSQR: An algorithm for sparse linear equations and sparse least squares, *ACM Trans. Math. Software* **8,** 43–71.

Schmandt, B., and F.-C. Lin (2014). *P* and *S* wave tomography of the mantle beneath the united states, *Geophys. Res. Lett.* **41,** no. 18, 6342–6349.

Villemaire, M., F. A. Darbyshire, and I. D. Bastow (2012). *P*-wave tomography of eastern North America: Evidence for mantle evolution from archean to phanerozoic, and modification during subsequent hot spot tectonism, *J. Geophys. Res.* **117,** no. B12302, doi: 10.1029/2012JB009639.

Wang, Y., and C. Tape (2014). Seismic velocity structure and anisotropy of the Alaska subduction zone based on surface wave tomography, *J. Geophys. Res.* **119,** no. 12, 8845–8865.

Scott Burdick
Department of Geology
University of Maryland
8000 Regents Drive
College Park, Maryland 20742 U.S.A.
sburdick@umd.edu

Frank L. Vernon
Vladik Martynov
Jennifer Eakins
Trilby Cox
Jonathan Tytell
Institute of Geophysics and Planetary Physics
University of California San Diego
9500 Gilman Drive
La Jolla, California 92093 U.S.A.

Taimi Mulder
Canadian Hazards Information Service
Natural Resources Canada
9860 West Saanich Road
British Columbia
Canada V8L 4B2

Malcolm C. White
Department of Earth Sciences
University of Southern California
3651 Trousdale Parkway
Los Angeles, California 90089 U.S.A.

Luciana Astiz
National Science Foundation
4201 Wilson Boulevard
Arlington, Virginia 22230 U.S.A.

Gary L. Pavlis
Department of Geological Sciences
Indiana University
1001 East 10th Street
Bloomington, Indiana 47405 U.S.A.

Robert D. van der Hilst
Department of Earth, Atmospheric, and Planetary Sciences
Massachusetts Institute of Technology
77 Massachusetts Avenue
Cambridge, Massachusetts 02139 U.S.A.